

Evidence of Eu^{2+} 4*f* electrons in the valence band spectra of EuTiO_3 and EuZrO_3

T. Kolodiazhnyi,^{1,a)} M. Valant,² J. R. Williams,³ M. Bugnet,⁴ G. A. Botton,⁴ N. Ohashi,⁵ and Y. Sakka⁶

¹National Institute for Materials Science, 1-1 Namiki, Tsukuba, Ibaraki 305-0044, Japan

²Materials Research Laboratory, University of Nova Gorica, Vipavska 13, 5000 Nova Gorica, Slovenia

³International Center for Young Scientists (ICYS), MANA, National Institute for Materials Science, 1-1 Namiki, Tsukuba, Ibaraki 305-0044, Japan

⁴Department of Materials Science and Engineering, McMaster University, Hamilton, Ontario L8S 4L7, Canada

⁵International Center for Materials Nanoarchitectonics, MANA, National Institute for Materials Science, 1-1 Namiki, Tsukuba, Ibaraki 305-0044, Japan

⁶National Institute for Materials Science, 1-2-1 Sengen, Tsukuba, Ibaraki 305-0047, Japan

(Received 20 July 2012; accepted 3 October 2012; published online 24 October 2012)

We report on optical band gap and valence electronic structure of two Eu^{2+} -based perovskites, EuTiO_3 and EuZrO_3 as revealed by diffuse optical scattering, electron energy loss spectroscopy, and valence-band x-ray photoelectron spectroscopy. The data show good agreement with the first-principles studies in which the top of the valence band structure is formed by the narrow Eu 4*f*⁷ electron band. The O 2*p* band shows the features similar to those of the Ba(Sr)TiO₃ perovskites except that it is shifted to higher binding energies. Appearance of the Eu^{2+} 4*f*⁷ band is a reason for narrowing of the optical band gap in the title compounds as compared to their Sr-based analogues. © 2012 American Institute of Physics. [<http://dx.doi.org/10.1063/1.4761933>]

I. INTRODUCTION

Recently several Eu^{2+} [4*f*⁷ (*S* = 7/2)] perovskite compounds have received a revised attention due to their magneto-dielectric and multiferroic properties.¹⁻³ Among them, EuTiO_3 is the most intensively studied compound. It shows tetragonal to cubic phase transition at around 300 K, whose exact temperature depends on the sample preparation conditions,⁴⁻⁶ and significant magneto-dielectric anomaly below $T_N \approx 5.5$ K.^{1,7,8} While the details of the magnetic ordering and the nature of the magneto-dielectric anomaly rightfully remain at the center of the debates,^{1,9-12} another important issue, that may pave the way for practical applications, is understanding of the electronic structure of the Eu^{2+} -based perovskites. According to the literature, most of the ATiO₃ perovskites with A = Ca²⁺, Sr²⁺, Ba²⁺ and Pb²⁺, show little contribution of the A-site cations to the low-energy part of the valence band.^{13,14} In contrast, the first-principles studies on EuTiO_3 suggest that the Eu^{2+} 4*f* electrons may form the highest occupied band in this compound. In addition, the magnitude of the on-site Coulomb interactions of the 4*f* electrons determines the width of the band gap.¹⁵ Hence, unlike the ATiO₃ perovskites whose optical band gap is formed by occupied O 2*p* and empty Ti 3*d* states, the band gap in EuTiO_3 is expected to form between the occupied Eu 4*f* and empty Ti 3*d* states.¹⁶ This difference may open up exciting opportunities in the field of magneto-optical applications involving, for example, EuTiO_3 -SrTiO₃ heterostructures with very large Faraday rotation effect.¹⁷

Another interesting aspect is realization of the *p*-type conductivity in Eu^{2+} perovskite family. While it is easy to

render SrTiO₃ or BaTiO₃ perovskites *n*-type by doping with donor ions or oxygen vacancies,¹⁸ it is almost impossible to achieve sizeable *p*-type conductivity at room temperature. In order to realize *p*-type conductivity in, e.g., Sr(Ba, Ca)TiO₃, substitution of Ti-cations with several acceptor-type ions, such as Al³⁺, Sc³⁺, etc., have been attempted in the past.^{19,20} Unfortunately, it was found that acceptor-type dopants are compensated by the oxygen vacancies or protons²¹ rather than by electron vacancies in the valence (oxygen 2*p*) band. At the same time, it does not seem to be very challenging to inject holes into the Eu^{2+} valence band by alloying EuTiO_3 with, e.g., EuScO_3 . However, before reporting on our attempts to achieve significant *p*-type conductivity in Eu^{2+} -based perovskites, it is important, first, to experimentally confirm the electronic valence band structure of the title compounds.

Here, we present diffuse optical absorption, electron energy loss, and x-ray photoelectron spectroscopy (XPS) data that show direct evidence that the Eu^{2+} 4*f* electrons form the highest occupied band in the EuTiO_3 and EuZrO_3 compounds. Due to localized nature of the 4*f* electrons, the band is rather narrow and is well separated from the lower-energy O 2*p* valence band in good agreement with the first-principles calculations.^{15,16}

II. EXPERIMENTAL

EuTiO_3 and EuZrO_3 were prepared from Eu_2O_3 , TiO₂ and ZrO₂ (99.9% pure). The stoichiometric mixtures were treated at 1100 °C (in case of EuTiO_3) and at 1300 °C (in case of EuZrO_3) for 20 h in pure hydrogen at a flow rate of 80 cm³/min, with intermediate re-grinding until black (EuTiO_3) and yellow (EuZrO_3) single phase products were

^{a)}Electronic mail: kolodiazhnyi.taras@nims.go.jp.

obtained. Phase purity was confirmed by powder x-ray diffraction (Rigaku Ultima III x-ray diffractometer with Cu K_α x-ray source). Magnetic susceptibility measurements using superconducting quantum interference device magnetometer (Quantum Design, MPMS) have confirmed that both EuTiO_3 and EuZrO_3 undergo magnetic phase transitions to AFM ground state at $T_N \approx 5.5$ K and 4.1 K, respectively. Magnetodielectric effect in EuZrO_3 compound has been reported elsewhere.³

The optical band gaps were calculated from the diffuse reflectance measurements by means of the diffuse reflectance spectroscopy. The spectra were recorded in the range of 250–800 nm with a UV-Vis spectrophotometer (Perkin Elmer, model λ 650 S) equipped with a 150 mm integrated sphere using spectralon as a reference material.

Electron energy loss spectroscopy (EELS) experiments were recorded in a transmission electron microscope (TEM) FEI Titan operated at 80 kV. With a monochromated electron beam and a 0.05 eV/channel dispersion, the energy resolution was 0.15–0.2 eV as measured by the full width at half maximum (FWHM) of the zero-loss peak. Bulk EuTiO_3 and EuZrO_3 samples were crushed in ethanol, deposited on a holey carbon grid, and baked at 100 °C for 2 h prior to insertion in the TEM in order to avoid contamination during the acquisition of the spectra.

XPS data were collected on dense ceramic pellets of EuTiO_3 and EuZrO_3 prepared by spark-plasma-sintering (SPS). Details of the SPS preparation of Eu^{2+} -based perovskites are reported elsewhere.³ The valence band structure were measured on a XPS Sigma Probe spectrometer (Thermo Scientific Co. Ltd., Yokohama, Japan) using monochromated Al K_α radiation (photon energy 1487 eV). The spectra were collected over a sufficient time to ensure a high signal to noise ratio. The samples were measured “as is” without any additional *in-vacuo* cleaning procedure. No significant charging effects were observed during spectra acquisition.

III. RESULTS AND DISCUSSION

According to Kubelka-Munk theory,²² the diffuse reflectance data were converted to absorbance coefficient $F(R_\infty)$

$$F(R_\infty) = \frac{(1 - R)^2}{2R} = \frac{\alpha}{S}, \quad (1)$$

where R is the reflectance, α and S are the absorption and scattering coefficients, respectively. The band gap (E_g) value and absorption coefficient are related through the following equation:

$$\alpha h\nu = \gamma(h\nu - E_g)^n, \quad (2)$$

where $h\nu$ is the photon energy and γ is a proportionality constant, $n = 1/2$ for a direct band gap semiconductor, or $n = 2$ for an indirect band gap semiconductor. The extrapolation of the linear part of the absorption edge in term of $[F(R_\infty)h\nu]^{1/n}$ on the photon energy axis gives the band gap value. In the case of the analyzed perovskites the extrapolation procedure has been successful for $n = 1/2$, which indicates that the perovskites are direct band gap semicon-

ductors (Fig. 1). Our band gap value for EuTiO_3 is 0.96 eV. This value is in good agreement with the room temperature ellipsometry data of $E_g = 0.93$ eV for unstrained EuTiO_3 thin film reported by Lee *et al.*²³ It is also in fair agreement with the optical absorption data of $E_g = 1.03$ eV for EuTiO_3 nanoparticles reported by Wei *et al.*²⁴ The 2.57 eV band gap value for EuZrO_3 reported here is consistent with the yellow color of the compound. It is also in good agreement with the recent optical data on EuTiO_3 , EuZrO_3 , and EuHfO_3 reported by Akamatsu.²⁵

A common feature is that both EuTiO_3 and EuZrO_3 offer optical band gap values that are significantly smaller than those of their Sr-based isomorphs. For example, SrTiO_3 and SrZrO_3 show band gaps of 3.3 and 5.6 eV, respectively.^{26,27} Bearing in mind an identical crystal structure, it is unlikely that such a big changes in E_g originate from the small differences in the Ti(Zr)–O bond length in the Sr- and Eu-based perovskites. Instead, it is most likely that the $\text{Eu}^{2+}4f$ electrons play a central role in defining the band gap in the latter perovskite family.

Figure 2 shows the EELS O-K edges of EuTiO_3 and EuZrO_3 . The near edge fine structures of the title compounds are very similar. The peaks A_1 and B_1 are attributed to the hybridization of O $2p$ states with the Ti $3d$ (Zr $4d$) states, split into t_{2g} (A_1) and e_g (B_1) sub-bands, and the Eu $5d$ states contribute significantly to C_1 and D_1 . Four main sets of peaks highlighted as $A_{1,2}$, $B_{1,2}$, $C_{1,2}$, and $E_{1,2}$ are identified in both EuTiO_3 and EuZrO_3 . Some differences, however, are observed in the two systems: the structure D_1 is not observed in EuZrO_3 , C_2 and E_2 in EuZrO_3 are located at lower energy than C_1 and E_1 in EuTiO_3 , respectively, and E_2 has a much weaker intensity than E_1 . In contrast, it is of interest to note that the O-K near edge fine structures of these Eu-containing perovskites are different from the ones in BaTiO_3 , for which Ba $4f$ states have been suggested to contribute to clearly distinguishable spectral features 11–13 eV above the edge onset.²⁹ No features in the fine structures in EuTiO_3 and EuZrO_3 can be attributed to a contribution of Eu $4f$ states and this observation indicates that there are no obvious

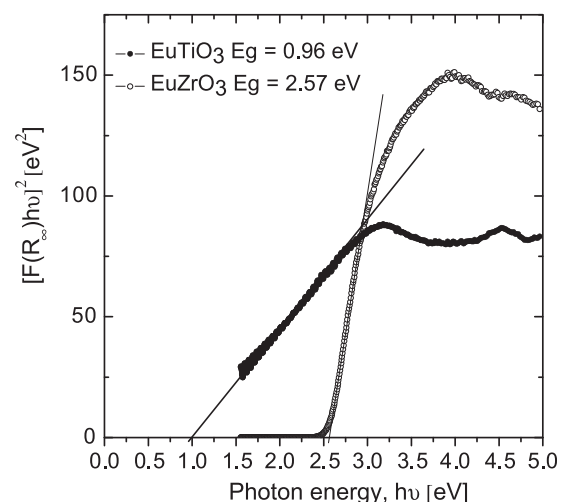


FIG. 1. Absorbance versus energy curves for EuTiO_3 and EuZrO_3 perovskites. The linear fit of $[F(R_\infty)h\nu]^2$ versus energy curve is shown with the solid lines.

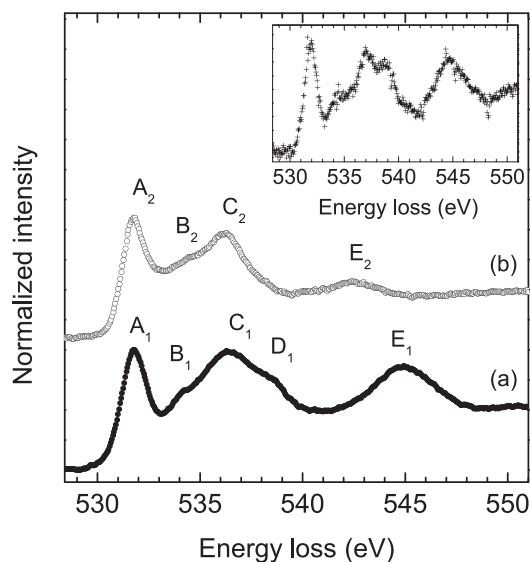


FIG. 2. Electron energy loss spectra of O-K edge of EuTiO_3 (a) and EuZrO_3 (b). The O-K edge of SrTiO_3 is added for comparison in the inset.²⁸ Spectra are aligned with respect to the peak A.

hybridization between O $2p$ and Eu $4f$ states in a 20 eV energy range above the Fermi level. Further information on the Eu $4f$ states with respect to the Fermi level cannot be directly inferred from these EELS spectra and we will now present XPS results to this end.

Figure 3 shows as-measured valence band XPS spectra of EuTiO_3 and EuZrO_3 referenced to zero Fermi energy, $E_F = 0$. Both perovskite compounds show qualitatively similar valence-band signature. Both spectra are characterized by a narrow, well-resolved, low-binding-energy peak attributed to the strongly localized $\text{Eu}^{2+} 4f$ electrons. The width of the $\text{Eu}^{2+} 4f$ peak is limited to the energy resolution of our XPS system. For better comparison, the XPS data were re-plotted in Fig. 4 with inelastic scattering removed and the binding energy (BE) referenced to the top of the valence band TVB $\equiv 0$. The TVB position was determined by extrapolating the steepest increase in the high-kinetic energy edge to zero, similar to the procedure reported by Hudson *et al.*³⁰ The derived position of the TVB is about 0.65 eV and 1.50 eV for

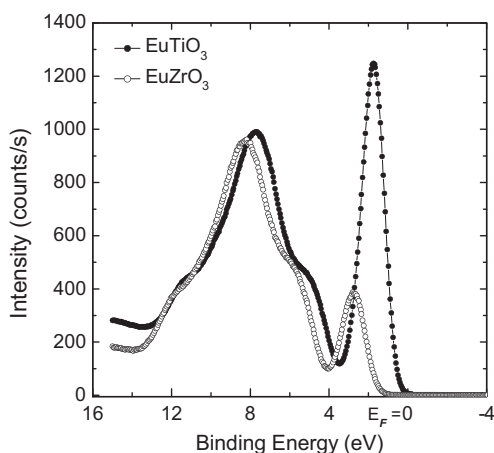


FIG. 3. Pristine valence band XPS data for EuTiO_3 and EuZrO_3 . The binding energy is referenced from $E_F \equiv 0$.

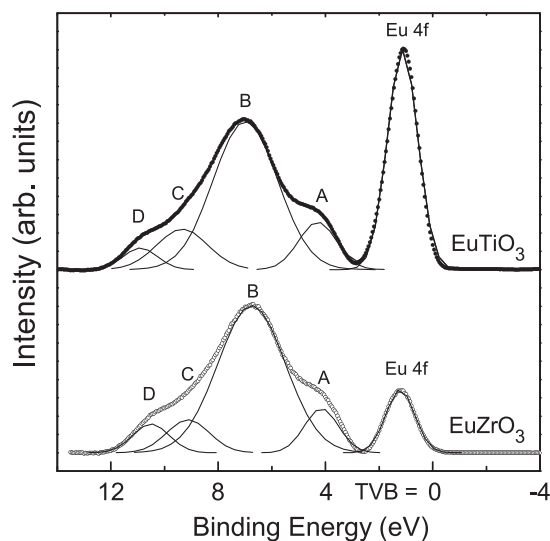


FIG. 4. Valence band XPS data for EuTiO_3 and EuZrO_3 with inelastic scattering background removed. The binding energy is referenced from top of the valence band TVB $\equiv 0$. The data were fitted to the sum of five Gaussian functions with parameters given in Table I.

EuTiO_3 and EuZrO_3 , respectively. Both values are larger than the half of the corresponding band gaps as determined by the diffuse optical absorption. This suggests that some band bending occurs at the surface and indicates that the Fermi level in both compounds is pinned by the in-gap surface states or chemisorbed molecules.

Because the samples were exposed to air atmosphere before mounting in the XPS chamber, one may expect that part of the Eu^{2+} ions will oxidize to form Eu^{3+} at the surface. Furthermore, small concentrations of Eu^{3+} in EuTiO_3 and EuZrO_3 samples were detected in the Mössbauer spectra.³¹ This should cause partial depopulation of the $\text{Eu}^{2+} 4f$ band and will pin the Fermi level at the onset of the valence band. However, the observed values of the TVB shift indicate an opposite trend where the Fermi level is shifted further up from the TVB. We conclude, therefore, that the pinning of the Fermi level is not caused by the possible Eu^{3+} states, but rather occurs due to surface contamination by chemisorbed molecules such as, CO, CO_2 , OH, etc., or partial reduction of Ti^{4+} (Zr^{4+}) ions. Indeed, we found an additional high-binding-energy peak of the O $1s$ level at 532.2 eV which provides a clear evidence that the both EuTiO_3 and EuZrO_3 surfaces contain significant amount of chemisorbed CO_2 .³²

As can be seen in Figures 3 and 4, in addition to the sharp $\text{Eu}^{2+} 4f$ peak, the valence band of EuTiO_3 and EuZrO_3 comprises a broad high-energy multi-structured band attributed to the O $2p$ states extending from 3 to 10 eV from the TVB. The overall profile of this O $2p$ band is in qualitative agreement with those observed in SrTiO_3 and BaTiO_3 perovskites. In order to determine the BE, the data were fitted to the sum of Gaussian functions and the BE values are reported in Table I together with the core electron levels. Also reported is the FWHM of the assigned peaks. The feature marked A in Fig. 4 centered at 4.9 and 5.7 eV for EuTiO_3 and EuZrO_3 , respectively, is assigned to the O $2p \sigma^0$ and π^0 non-bonding bands, since they do not involve

TABLE I. XPS BEs and their full width at half maximum for EuTiO₃ and EuZrO₃. The binding energies (in eV) quoted in this table are referenced to the pinned Fermi level, $E_F = 0$.

Level	EuTiO ₃		EuZrO ₃	
	BE	FWHM	BE	FWHM
Eu ²⁺ 4 <i>f</i>	1.8	1.1	2.7	1.1
VB feature A	4.9	1.4	5.7	1.3
VB feature B	7.6	2.4	8.3	2.5
VB feature C	10.0	1.9	10.6	1.6
VB feature D	11.6	1.3	12.0	1.4
Ti 2 <i>p</i> $\frac{3}{2}$	459.3	1.3		
Ti 2 <i>p</i> $\frac{1}{2}$	465.1	2.3		
Zr 3 <i>d</i> $\frac{5}{2}$			183.4	1.6
Zr 3 <i>d</i> $\frac{3}{2}$			185.8	1.5
O 1 <i>s</i> bulk	530.7	1.7	531.3	1.7
O 1 <i>s</i> contaminant	532.2	1.8	533.2	1.8

hybridization with the Ti(Zr) *d*-orbitals. High-energy features B and C in Fig. 4 are assigned to the π - and σ -type bonding bands, respectively. They involve admixture of Ti(Zr) ion and oxygen orbitals.³³

In addition to the oxygen ligand contribution to the valence band, in both compounds, we have also detected the feature marked D in Fig. 4. One of the possible origins of this feature is the bonding interactions of the oxygen 2*p* and Eu 5*d* orbitals reported in the first-principles calculations.^{15,16} However, the strength of these interactions is very weak and can hardly account for a noticeable intensity of feature D. It may be also mentioned that the valence-band structure of the EuTiO₃ thin film probed by hard x-ray photoelectron spectroscopy show no evidence of the D feature.¹² It is more plausible, therefore, that the feature D in our samples originates from the surface contamination. Indeed, Robey *et al.* reported contamination-induced intensity at a BE = 11 eV in resonant photoelectron spectroscopy studies on BaTiO₃, R_{1-x}Ba_xTiO₃, R = Y, La, Nd, and Nd_{1-x}Sr_xTiO₃.^{34,35} More accurate measurements of the valence band spectra are necessary in order to clarify the origin of the feature D in both EuTiO₃ and EuZrO₃.

One of the points that requires further studies is a factor of 3 enhancement in the intensity of the Eu²⁺ 4*f* peak in EuTiO₃ as compared to that in EuZrO₃ (see, e.g., Fig. 3). Because the soft x-ray photoelectron spectroscopy is surface-sensitive technique, we speculate that the large difference in the Eu²⁺ 4*f* signal may be partially explained by the different surface conditions of the samples. From the point of view of magnetic exchange interactions, future studies may require resonant photoelectron spectroscopy at the Ti 3*p* threshold energy in order to reveal any Eu²⁺ superexchange interactions via Ti 3*d* states as was recently proposed by Akamatsu *et al.*¹² The possible admixture of Ti 3*d* states in the Eu 4*f*⁷ electron band may also explain the large difference in the XPS intensity of the Eu 4*f*⁷ peak in the EuTiO₃ and EuZrO₃ samples found in this study. Indeed, the enhanced Eu²⁺ 4*f* signal in EuTiO₃ is in qualitative agreement with a factor of 27 enhancement in the magneto-

dielectric coupling constant in EuTiO₃ as compared to that of EuZrO₃.³

In conclusion, we reported on optical band gap and valence electronic structure of two Eu²⁺-based perovskites, EuTiO₃ and EuZrO₃ as revealed by diffuse optical scattering, EELS, and valence-band XPS. In agreement with first-principles studies, both compounds show significantly smaller band gap as compared to their Sr-based counterparts. The top of the valence band of the former perovskites is comprised of the narrow-band formed by the Eu 4*f*⁷ electrons. It is this band that causes the narrowing of the optical band gap in Eu²⁺-based perovskites. Injecting holes into the valence band by acceptor doping may be a viable path to introduce *p*-type conductivity in these compounds. However, the localized nature of the Eu 4*f*⁷ electrons may pose challenge in realization of significant *p*-type conductivity in the title compounds.

ACKNOWLEDGMENTS

Part of this work was supported by Grant-in-Aid for Scientific Research C 21560025 from MEXT Japan provided to T. Kolodiazhnyi.

- ¹T. Katsufuji and H. Takagi, *Phys. Rev. B* **64**, 054415 (2001).
- ²J. H. Lee *et al.*, *Nature* **466**, 954–959 (2010).
- ³T. Kolodiazhnyi, K. Fujita, L. Wang, Y. Zong, K. Tanaka, Y. Sakka, and E. Takayama-Muromachi, *Appl. Phys. Lett.* **96**, 252901 (2010).
- ⁴A. Bussmann-Holder, J. Köhler, R. K. Kremer, and J. M. Law, *Phys. Rev. B* **83**, 212102 (2011).
- ⁵M. Allieta, M. Scavini, L. J. Spalek, V. Scagnoli, H. C. Walker, C. Panagopoulos, S. S. Saxena, T. Katsufuji, and C. Mazzoli, *Phys. Rev. B* **85**, 184107 (2012).
- ⁶V. Goian, S. Kamba, O. Pachrová, J. Drahoukoupil, L. Palatinus, M. Dušek, J. Rohlíček, M. Savinov, F. Laufek, W. Schranz, A. Fuiith, M. Kachlík, K. Maca, A. Shkabko, L. Sagarna, A. Weidenkaff, and A. A. Belik, *Phys. Rev. B* **86**, 054112 (2012).
- ⁷S. Kamba, D. Nuzhnyy, P. Vaněk, M. Savinov, K. Knížek, Z. Shen, E. Santavá, K. Maca, M. Sadowski, and J. Petzelt, *Europhys. Lett.* **80**, 27002 (2007).
- ⁸V. Goian, S. Kamba, J. Hlinka, P. Vaněk, A. A. Belik, T. Kolodiazhnyi, and J. Petzelt, *Eur. Phys. J. B* **71**, 429 (2009).
- ⁹Q. Jiang and H. Wu, *J. Appl. Phys.* **93**, 2121 (2003).
- ¹⁰C. J. Fennie and K. M. Rabe, *Phys. Rev. Lett.* **97**, 267602 (2006).
- ¹¹V. V. Shvartsman, P. Borisov, W. Kleemann, S. Kamba, and T. Katsufuji, *Phys. Rev. B* **81**, 064426 (2010).
- ¹²H. Akamatsu, Y. Kumagai, F. Oba, K. Fujita, H. Murakami, K. Tanaka, and I. Tanaka, *Phys. Rev. B* **83**, 214421 (2011).
- ¹³L. F. Mattheiss, *Phys. Rev. B* **6**, 4740–4753 (1972).
- ¹⁴E. Heifets, E. Kotomin, and V. A. Trepakov, *J. Phys.: Condens. Matter* **18**, 4845–4851 (2006).
- ¹⁵R. Ranjan, H. S. Nabi, and R. Pentcheva, *J. Phys.: Condens. Matter* **19**, 406217 (2007).
- ¹⁶R. Ranjan, H. S. Nabi, and R. Pentcheva, *J. Appl. Phys.* **105**, 053905 (2009).
- ¹⁷J. L. M. van Mechelen, D. van der Marel, I. Crassee, and T. Kolodiazhnyi, *Phys. Rev. Lett.* **106**, 217601 (2011).
- ¹⁸T. Kolodiazhnyi, *Phys. Rev. B* **78**, 045107 (2008).
- ¹⁹T. Higuchi, T. Tsukamoto, N. Sata, M. Ishigame, Y. Tezuka, and S. Shin, *Phys. Rev. B* **57**, 6978–6983 (1998).
- ²⁰X. Guo, C. Pithan, C. Ohly, C.-L. Jia, J. Dornseiffer, F.-H. Haegel, and R. Waser, *Appl. Phys. Lett.* **86**, 082110 (2005).
- ²¹N. Sata, K. Hiramoto, M. Ishigame, S. Hosoya, N. Niimura, and S. Shin, *Phys. Rev. B* **54**, 15795–99 (1996).
- ²²P. Kubelka and F. Munk, *Z. Tech. Phys.* **12**, 593 (1931).
- ²³J. H. Lee *et al.*, *Appl. Phys. Lett.* **94**, 212509 (2009).
- ²⁴T. Wei *et al.*, *Appl. Surf. Sci.* **257**, 4505–4509 (2011).

- ²⁵H. Akamatsu, K. Fujita, H. Hayashi, T. Kawamoto, Y. Kumagai, Y. Zong, K. Iwata, F. Oba, I. Tanaka, and K. Tanaka, *Inorg. Chem.* **51**, 4560–4567 (2012).
- ²⁶J. L. M. van Mechelen, D. van der Marel, C. Grimaldi, A. B. Kuzmenko, N. P. Armitage, N. Reyren, H. Hagemann, and I. I. Mazin, *Phys. Rev. Lett.* **100**, 226403 (2008).
- ²⁷Y. S. Lee, J. S. Lee, T. W. Noh, D. Y. Byun, K. S. Yoo, K. Yamaura, and E. T. Muromachi, *Phys. Rev. B* **67**, 113101 (2003).
- ²⁸G. Radtke and G. A. Botton, *Microsc. Microanal.* **10**(S2), 852–853 (2004).
- ²⁹G. Radtke, C. Maunders, A. Saúl, S. Lazar, H. J. Whitfield, J. Etheridge, and G. A. Botton, *Phys. Rev. B* **81**, 085112 (2010).
- ³⁰L. T. Hudson, R. L. Kurtz, S. W. Robey, D. Temple, and R. L. Sokbauer, *Phys. Rev. B* **47**, 1147 (1993).
- ³¹Y. Zong, K. Fujita, H. Akamatsu, S. Murai, and K. Tanaka, *J. Solid State Chem.* **183**, 168 (2010).
- ³²J. D. Baniecki, M. Ishii, K. Kurihara, K. Yamanaka, T. Yano, K. Shinozaki, T. Imada, K. Nozaki, and N. Kin, *Phys. Rev. B* **78**, 195415 (2008).
- ³³T. Wolfram and Ş. Ellialtıođlu, *Electronic and Optical Properties of d-Band Perovskites* (Cambridge University Press, Cambridge, 2006), p. 14.
- ³⁴S. W. Robey, L. T. Hudson, C. Eylem, and B. Eichorn, *Phys. Rev. B* **48**, 562–568 (1993).
- ³⁵S. W. Robey, L. T. Hudson, V. E. Henrich, C. Eylem, and B. Eichhorn, *J. Phys. Chem. Solids* **57**, 1385–1391 (1996).